Journal of the Korean Nuclear Society
Volume 33, Number 6, pp.619~625, December, 2001

FIV Analysis for a Rod Supported by Springs at Both Ends

H. S. Kang, K. N. Song, H. K. Kim, and K. H. Yoon

Korea Atomic Energy Research Institute,
150 Dukjin-dong, Yusong-gu, Taejon 305-353, Korea
hskang@nanum.kaweri.re.kr

(Received May 24, 2001)

Abstract

An axial-flow-induced vibration model was proposed for a rod supported by two translational springs at both ends. For developing the model, a one-mode approximation was made based on the assumption that the first mode was dominant in vibration behavior of the single span rod. The first natural frequency and mode shape functions for the flow-induced vibration, called the FIV, model were derived by using Lagrange' s method. The vibration displacements at reactor conditions were calculated by the proposed model for the spring-supported rod and by the previous model for the simple-supported(SS) rod. As a result, the vibration displacement for the spring-supported rod was larger than that of the SS rod, and the discrepancy between both displacements became much larger as flow velocity increased. The vibration displacement for the spring-supported rod appeared to decrease with the increase of the spring constant. As flow velocity increased, the increase rate of vibration displacement was calculated to go linearly up, and that of the rod having the short span length was larger than that of the rod having the long span length although the displacement value itself of the long span rod was larger than that of the short one.

Key Words : fuel rod, FIV, spring support, natural frequency, mode shape, spacer grid

1. Introduction

PWR fuel rods are exposed to reactor coolant of high flow velocity. It is known that the vibration of the fuel rod(FR) is generated by the coolant flow, and the fretting-wear by the vibration is frequently found on the surface of it. This problem of the FR is not because of fluidelastic instability that cause excessive vibration and failure in short time but because of turbulence-induced excitation that generates small amplitude[1] and may cause long-term fretting-wear damage. The fretting wear by this sub-critical vibration is generally accepted as a root cause of a fuel rod failure that is not yet known well. Since the FIV obviously generates the relative motion between the FR and the spacer grid, that can lead to fretting damage of the FR, it is very important to understand what the actual vibration behavior of the fuel rod

supported by spacer grids is. The spacer grid has several springs in a cell in order to support the fuel rod flexibly. Therefore, the supporting method for the fuel rod is actually not a simple support but a spring support. It was reported that the spring constant of the spacer grid gave a significant effect to the modal parameters of the FR[2].

However, most works on FIV of the FR were associated with the SS cylinder. In this study, therefore, the spring support effect on the FIV of the cylinder was surveyed as compared with the SS. In addition, the span length effects were investigated for that of the PWR fuel.

In order to derive the FIV model for the spring-supported cylinder, the author' s previous work[3] was completely accepted, in which a procedure was described to solve the random vibration problem of the cylinder subjected to the randomly fluctuating pressure acting on the cylinder surface by axial flow. The cylinder vibration mode was obtained by using Lagrange' s method based on the single mode(1st mode) approximation. For the numerical calculations, the spring constants were selected within the range of those of the commercial spacer grid springs, and the material properties of the cylinder and flow conditions for the PWR reactor were used.

2. Mathematical Model and Numerical Calculation

2.1. Mathematical Model

The following Equation Of Motion(EOM) is basically used with the exception of the axial force, which was proposed by the previous study[3].

$$EI\frac{\partial^4 y}{\partial x^4}+(m_f V^2)\frac{\partial^2 y}{\partial x^2}+C\frac{\partial y}{\partial t}+M\frac{\partial^2 y}{\partial t^2} = q(x,t) \tag{1}$$

Where m_f is the mass of fluid entrained by the cylinder, so-called added mass of fluid, which can be derived based on the theory of potential flow[4].

$C\frac{\partial y}{\partial t}$ is the viscous damping force that was equated to the sum of the forces Fs , defined as in the previous study[3].

$$\begin{aligned} F_s = &-\frac{1}{2}\rho DV^2 C_f \frac{\partial^2 y}{\partial x^2}\left(\frac{L}{2}-x\right) \\ &+2m_f V\frac{\partial^2 y}{\partial x\partial t}+\rho DV^2 C_f\frac{\partial y}{\partial x} \\ &+\frac{1}{2}\rho DV C_f\frac{\partial y}{\partial t} \\ &+\frac{1}{2}\rho DC_D\left|\frac{\partial y}{\partial t}\right|\cdot\frac{\partial y}{\partial t} \end{aligned} \tag{2}$$

The C_f and C_D in Eq. (2) are the profile and skin drag respectively for a rod. Since it is well known that the rod in axial flow is a weak-damping system, the damping term in equation (1) can be neglected for simplicity in obtaining natural frequencies and mode shapes.

Let' s consider a cylinder having uniform mass supported by two springs at the both ends as shown in Fig 1.

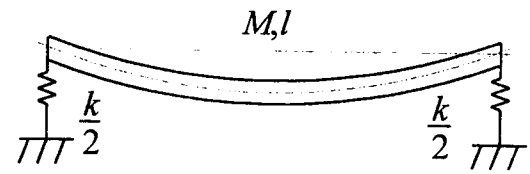

Fig. 1. A Rod Supported by Equal Springs at Both Ends

The deflection equation of the cylinder was assumed to be

$$y(x,t)=\phi_1(x)q_1(t)+\phi_2(x)q_2(t) \tag{3}$$

The spatial equations $\phi_1 = \sin(\pi x/l)$and $\phi_2=1.0$

could be chosen for the equation (3).

Using Lagrange' s equation, the following were obtained.

$$\ddot{q}_1 + \frac{4}{\pi}\ddot{q}_2 + \omega_{11}^2 q_1 = 0 \tag{4}$$

$$\frac{2}{\pi}\ddot{q}_1 + \ddot{q}_2 + \omega_{22}^2 q_2 = 0 \tag{5}$$

where $\omega_{11}{}^2 = \left(\frac{\pi}{l}\right)^2 \frac{m_f V^2}{M} + \left(\frac{\pi}{l}\right)^4 \frac{EI}{M}$;

natural frequency of the beam on rigid supports

$\omega^2_{22} = \frac{k}{m}$; natural frequency of rigid beam on springs

Solving these equations, the natural frequency for the cylinder supported on the two springs can be obtained from the equations as follows:

$$\omega_n{}^2 = \omega_{22}^2 \frac{\pi^2}{2}\left\{\frac{(T+1) \pm \sqrt{(T-1)^2 + \frac{32}{\pi^2}T}}{\pi^2 - 8}\right\} \tag{6}$$

where, $T = \left(\frac{\omega_{11}}{\omega_{22}}\right)^2$ (7)

The deflection equation can be taken as follows;

$$y(x,t) = \phi(x)q(t) = (b + \sin\frac{\pi x}{l})q(t) \tag{8}$$

where,

$$b = \frac{\pi}{8}\left\{(T-1) \mp \sqrt{(T-1)^2 + \frac{32}{\pi^2}T}\right\} \tag{9}$$

2.2. Natural Frequency and Mode Shape Comparison with SS Rod and Spring-Supported Rod

For numerical calculation, material properties and geometry of the fuel rod, and spring constant range of the commercial spacer grid springs were used as summarized in Table 1. The fuel rod was assumed to be in the PWR reactor. Thus, the temperature and velocity range of the coolant was

Table 1. Material and Geometry Data

Name	Property	Value(310℃)
Rod	EI	14.03 N/m^2
	Mass per length	0.728 kg/m
	Span length	0.522/0.62 m
	O.D / I. D	9.5 / 8.22 mm
Spring	Constant	50~400 kN/m

Table 2. 1st Natural Frequency of SS and Spring Support(flow V= 6 m/s)

Case		1st Natural Frequency (Hz)	
		Span L =0.52m	Span L =0.62m
SS-SS		25.35	17.98
Spring Support	K= 50 kN/m	23.52	17.18
	K= 200 kN/m	24.86	17.78
	K= 400 kN/m	25.10	17.88

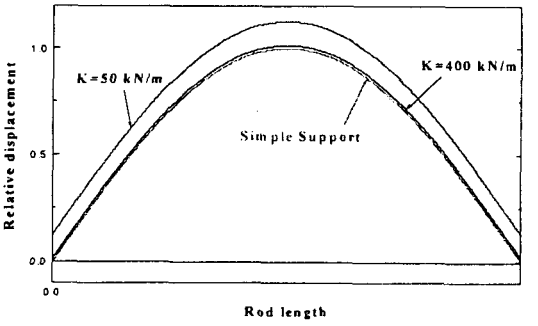

Fig. 2. First Mode Shapes of the SS Rod and the Spring-supported Rod

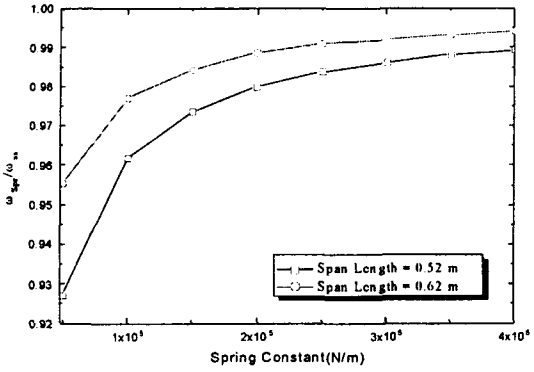

Fig. 3. Spring Constant Versus Frequency Ratio

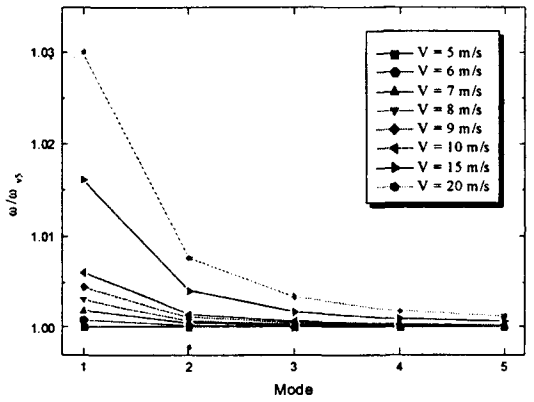

Fig. 4. Flow Velocity Versus Natural Frequency Ratio

assumed to be 310 ℃, and 5 to 8 m/s. Since this calculation was based on the single mode approximation, only the first mode shape was calculated and compared as shown in Fig. 2. The calculation results were summarized in Table 2. Natural frequency in the case of the spring support appeared to increase gradually up to that of SS with the increase of the spring constant. The natural frequency variation of the spring-supported rod was shown in Fig. 3 along with the increase of the spring constant.

The longer rod having a span length of 0.62 m converged faster than that of 0.52 m. Theoretically, the SS can be considered as the spring support by the infinite spring constant. Therefore, the calculation results for the spring-supported rod were judged to be reasonable.

Flow velocity was known as a parameter giving effect to natural frequencies and mode shapes. The influence of flow velocity could be guessed by the flow velocity term in equation (1). This effect, however, turned out to be insignificant as depicted in Fig. 4.

Even though flow velocity had the biggest effect on the fundamental mode, it turned out to be 3% at most when its velocity was 20 m/s.

2.3. Flow-induced-vibration Analysis

The response of the cylinder to the turbulence axial flow was derived in the previous study[3]. The result is written as follows;

$$\Phi_{yy}(\xi,\xi',\omega) = 4d^2 \sum_{m=1}^{\infty}\sum_{n=1}^{\infty}(\phi(\xi)\phi(\xi')\, H_m(\omega) H_n^*(\omega)\chi^2\, \psi(\omega)\, Jn^2) \quad (10)$$

where,

Φ_{yy}; Displacement Power Spectral Density (Displacement PSD)

$$H_n = \frac{1}{\sqrt{EI(\eta)^4 - m_f V^2(\eta)^2 - M\omega^2 + i2\zeta M\omega\omega_n}}$$

Frequency Response Function(FRF)

$n = 1$

$$\eta = \frac{n\pi}{l}$$

H^*_n; Conjugate of H_n

Jn; Joint acceptance[3 and5]

$$\chi^2 = \frac{1}{4}\int_0^{2\pi}\int_0^{2\pi}(Exp\left[-0.275\frac{\omega d}{U}\left|\theta-\theta'\right|\right] \cos\theta' \cos\theta)\, d\theta' d\theta$$

U; Convection Velocity[6]

ψ; Power spectral density of wall pressure[3]

$\zeta = \frac{C}{2M\omega_n}$; Critical Damping Ratio

ω; Frequency

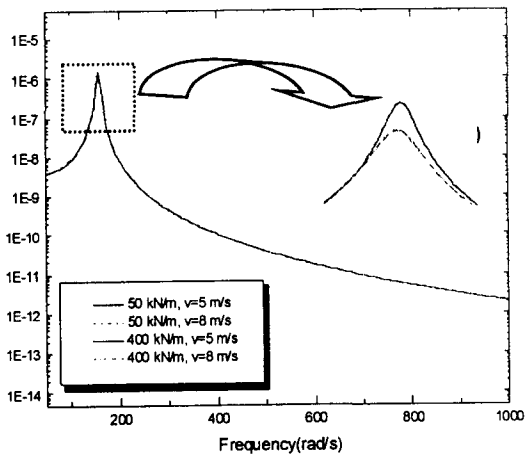

Fig. 5. Frequency Response Function for Spring Support

Vibration displacement of the rod can be obtained by integrating equation (10) from zero to infinite on the frequency domain. The damping model and power spectral density of wall pressure discussed in the previous study[3] was used.

The frequency response function multiplied by its conjugate was calculated according to spring stiffness, and its results are illustrated in Fig. 5.

3.4. Numerical Calculation Results

Using the derived equations in section 2.1 and the data in Table 1 and 2, the displacement PSDs for both the SS rod and the spring-supported rod were calculated for flow velocity of 5 m/s and 8 m/s, and their results were depicted in Fig. 6.

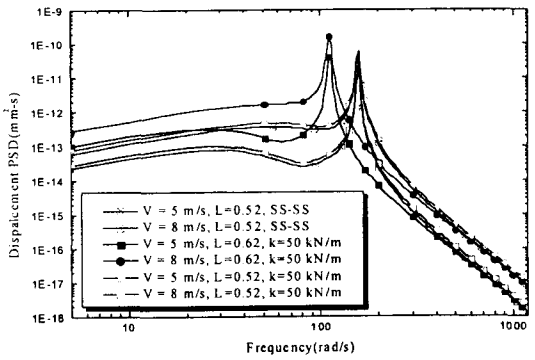

Fig. 6. Displacement PSD of Both SS Rod and Spring-support Rod

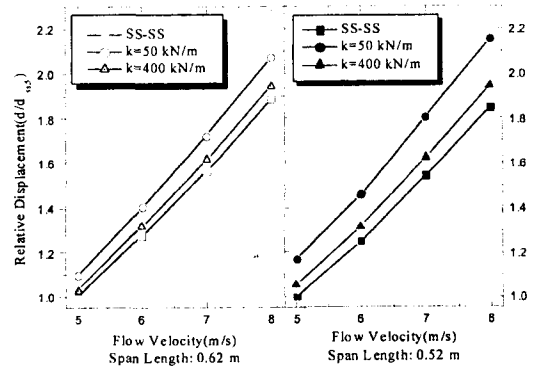

Fig. 7. Vibration Displacement Ratio of a Rod as a Function of Mean Flow Velocity

The level of the displacement PSD goes up as the flow velocity increases, the spring constant decreases, and rod length(span length) increases while the resonant frequencies seem to have no change. The PSD level of the spring-supported rod is slightly higher than that of the SS rod at the same flow velocity. The highest PSD level was obtained at the combined parameters such as the flow velocity of 8 m/s, the rod length of 0.62 m and the spring constant of 50 kN/m, so-called a soft spring.

The vibration displacement of the rod in axial flow can be obtained by integrating the PSD shown in Fig. 6 from 0(zero) to infinite theoretically. However, as reported not only in the author's previous study[3] but in many papers, it was believed that a one-mode(1st mode) approximation would be enough to predict the rod vibration from the actual engineering point of view. Therefore, in this study, it was decided that the integration range from 0(zero) to 800 rad/s (127 Hz) would be adopted to obtain the vibration displacement. The displacements obtained in that way were illustrated in Fig. 7. The results came up to the expectation that the maximum displacement would be obtained in the case of the cylinder being exposed at the flow velocity of 8 m/s, the rod length of 0.62 m and supported on a spring constant of 50 kN/m, which was the highest flow velocity, the longest span length and softest spring of all the cases. All the results were normalized by that of the SS rod at 5 m/s velocity. The softer the support spring is, the larger the vibration displacement is at the same flow velocity. As it were, when the flow velocity is 5m/s, the displacement difference between the SS rod and the rod supported by the 50 kN/m and 400 kN/m is 16.8% versus 5.3% for the rod of 0.52 m, and that difference goes gradually up to 116% versus 94% when the flow velocity becomes 8 m/s. The difference increases from 11.5 % to 22 % as flow velocity increases from 5 m/s to 8 m/s. this means that the spring effect becomes stronger as the flow velocity increases without regard to the rod length. However, the ratio of the displacement discrepancy between the rod length of 0.52 and 0.62 m at the same flow velocity is not equal. The increase rate of the displacement ratio of the shorter rod is higher although its vibration displacement value is almost 50% smaller than that of the longer one.

3. Conclusions

An axial-flow-induced vibration(FIV) model was proposed for a rod supported by two translational springs at both ends. The first natural frequency and mode shape functions for the FIV model were derived by using Lagrange's method based on the single mode approximation. The vibration displacement was calculated by the proposed model for the spring-supported rod of which the span lengths were 0.52 m and 0.62 m respectively, and the results were compared with those of the SS rod. It was concluded that the vibration displacement for the spring-supported rod was larger than that of the SS rod, and the displacement decreased with an increase of the spring constant, and the displacement of the rod length of 0.62 m was 50% as large as that of 0.52 m for most flow velocities. Although the vibration displacement due to axial flow appeared to be clearly dominated by the flow velocity and was considered to be small in quantity, in case of the PWR rod supported by the soft spring, 20% more displacement than the SS rod may possibly be appreciated in the range of the flow velocity of 5 to 8 m/s, which is known to be the velocity range of the PWR reactor coolant.

Acknowledgement

This project has been carried out under the nuclear R&D program by MOST.

References

1. M.P. Paidoussis, "Fluidelastic Vibration of Cylinder Arrays in Axial and Cross Flow-State

of the Art", J. of Sound and Vibration, 76, pp. 329~360 (1981).

2. H.S.Kang, et al., "A Study on the Vibrational Behavior of the Fuel Rods Continuously Supported by a Rotary and Bent Spring System, "Korea Sound and Vibration Society, May 1998, pp. 454~460 (1998)
3. H.S. Kang, et al., "A Study on the Axial-flow-induced Vibration of Fuel Rod,' Tansactions of the 15th International Conference on SMiRT, Vol. 2, pp. 341~ 348, Seoul, Korea, August, 15-20 (1999).
4. R. D. Blevins, "Flow-induced Vibration," 2nd ed., pp. 20~25, Van Nostrand Reinhold, New York (1990).
5. S.S. Chen and W. Wambsganss, "Parallel-flow-induced vibration of fuel rods," Nuclear Engineering and Design 18, pp.253~278 (1972).
6. G.M. Corcos, "The Structure of the Turbulent Pressure Field in Boundary-layer Flows," J. of Fluid Mechanics, Vol. 18, pp. 353~358 (1962).